Inductive Communication and Localization Method for Wireless Sensors in Photobioreactors

David Demetz

UMIT - Private University for Health Sciences,
Medical Informatics and Technology
Hall in Tirol, Austria
Email: david.demetz@umit.at

Alexander Sutor

UMIT - Private University for Health Sciences,
Medical Informatics and Technology
Hall in Tirol, Austria
Email: alexander.sutor@umit.at

***Abstract*—A method for an inductive communication and localization system for wireless sensors in internally illuminated photobioreactors is presented here. The communication is implemented through an on-off switched hartley-oscillator where its inductance is used as transmitting coil for the wireless sensor data. As modulation technique, the on-off keying is used. The magnetic field of the transmitting coil is sensed from outside the reactor with special designed receivers in order to evaluate the magnetic field components of the transmitting coil in all three spatial directions at one position. This enables the localization of the transmitting coil and thus the localization of the wireless sensor. A prototype has been implemented and test measurements performed with a two receiver setup. Additionally simulations were performed in order to see the accuracy improvement of the localization by using more receivers.**

Keywords–wireless sensors; inductive localization; inductive communication.

I. INTRODUCTION

We already presented a wireless internal illumination system for photobioreactors in past [1]. The internal illumination of photobioreactors is needed due to the low penetration depth of light in the reactor medium. This novel illumination system consists of small wireless, inductively powered luminous spheres called Wireless Light Emitters (WLEs). The fact that the WLEs have the same overall density as water enables them to float in the reactor medium. The external magnetic field used to power the WLEs is generated by field coils driven by a class-E amplifier. The frequency of the alternating field is 178 kHz. The archived flux density in the photobioreactor amounts to approx. B = 1 mT [1]–[3].

For a better control of the processes inside the reactor, a further step is the measurement of crucial parameters such as temperature, salinity or oxygen concentration using wireless traceable sensors. Currently used setups use fixed sensors where drill holes or other reactor modifications are needed to install them. Using wireless sensors, those modifications are no more needed. In a similar project [4] they presented battery powered wireless sensor-spheres for bioreactors, which transmit their measured values using the 433 MHz frequency band. The sensors in our project will be powered through the inductive link used to power the WLEs. The traceability enables a spatial resolution of the measured values. The communication link is implemented as a separate inductive link with a carrier frequency of 297 kHz and is therefore 1.66 times higher than the frequency of the power supply field. This is to avoid interferences caused by harmonics. The mathematical description of the magnetic dipole field is used to solve the traceability task. Thereby the magnetic field of the data transmitting coil is measured in order to calculate the transmitter position. We already presented the design of our transmitter in another publication [5]. Now, we will take a closer look at the traceability task and the receiver design.

In Section II the chosen data transmission method and the used modulation technique are described. The model equations used to describe the magnetic field of a coil in order to derive the equation system used to solve the localization task are also presented in Section II. The receiver architecture, the receiver electronics, the measurement setup and the receiver arrangement are presented in Section III. In Section IV the results of preliminary localization measurements are shown. We also performed simulations to analyze the improvement in the localization accuracy by using more then two receivers. The simulation method and the simulation results are listed in Section V followed by the conclusion in Section VI.

II. PRELIMINARY WORK

For the sensor data transmission and for solving the localization task the well defined properties of magnetic fields are used.

A. Data Transmission

The propagation characteristics of magnetic fields do not differ between water and air due to their similar magnetic permeabilities [6]. The radio frequency data transmission, on the other hand suffers from high attenuations in underwater environments [7]. Common used methods for underwater data exchange systems are also the acoustic and the optical data transmission [8]–[10]. We choose the magneto-inductive data transmission since the acoustic and the optical methods are not well suited for our aim. The optical method would not be feasible due to the many obstacles in the reactor; for example the WLEs or the algae. The acoustic method is unsuitable due to the physical separation between transmitter and receiver by the reactor wall. As modulation technique, in order to overlap a digital signal on a carrier wave, we use the on-off keying. This is implemented by switching a hartley-oscillator on and off. The sensor data stream is currently simulated with a bit-generator. The bit-generator is a square wave generator

 ISBN: 978-1-61208-819-8

based on the integrated circuit LM555. The high level of the generated square wave represents the 1-bit and the low level the 0-bit. This signal is used as control signal to switch the hartley-oscillator on and off.

B. Inductive Localization

The magnetic field of a coil with N turns modelled as a dipole field can be described by its radial (H_r) and tangential (H_t) components like shown in (1) and (2), where A is the cross section area of the coil, $I = i\cos(\omega t)$ the exciting current, ϱ is the radial distance from the coil centre and ζ the off axis angle [11].

$$H_r = \frac{NIA}{2\pi\varrho^3}\cos\zeta \tag{1}$$

$$H_t = \frac{NIA}{4\pi\varrho^3}\sin\zeta \tag{2}$$

Equation (3) is the coupling equation between a transmitter and a receiver where both of them have the same orientation ($\vec{e}_{x-rx} = \vec{e}_{x-tx}$ and $\vec{e}_{y-rx} \parallel \vec{e}_{y-tx}$ and $\vec{e}_{z-rx} \parallel \vec{e}_{z-tx}$) [11].

$$\vec{f}_{rx} = \left(\frac{C}{\varrho^3}\right)\mathbf{S}\vec{f}_{tx} \tag{3}$$

$$\mathbf{S} = \mathrm{diag}(1\ -0.5\ -0.5) \tag{4}$$

In (3), the transmitter signal vector is referred to as $\vec{f}_{tx}$ and the receiver signal vector as $\vec{f}_{rx}$. ϱ is the distance between them and C is a constant factor derived from the receiver parameters (coil properties, signal gain). To simplify the localization task, the transmitter coil is assumed to be always aligned with a global z-coordinate like shown in Figure 1. By measuring the x-, y- and z-components of the magnetic field at one position it's possible to calculate a direction vector $\vec{r}$ defined by the angles α and β (see Figure 1) that points from the measuring point to the transmitter position. By measuring the x, y and z magnetic field components at two or more defined positions the localization of the transmitter coil can be calculated by finding the point where the direction vectors of all measuring points comes closest to each other (ideally the intersection). Expanding (3) with the rotation matrix around the z-axis ($\mathbf{T}_\alpha$)

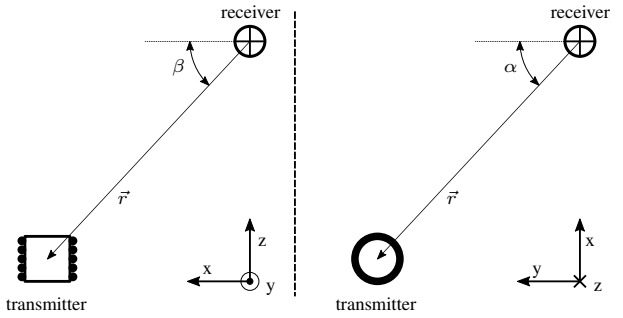

Figure 1. Transmitter-receiver alignment

and the rotation matrix around the y-axis ($\mathbf{T}_\beta$), we get (5), which describes the coupling between the transmitter and a receiver in our setup. Solving (5) for the angles α and β enables us to calculate the direction vector $\vec{r}$. Since we do only transmit in z-direction the transmitter signal vector $\vec{f}_{tx} = [0\ 0\ a]^T$ is an unknown value a in z-direction. The value is assumed as unknown since the transmitting power depends on the actual position of the transmitting coil in the photobioreactor. $\vec{f}_{rx}$ contains the measured field components in x- y- and z-direction.

$$\vec{f}_{rx} = \left(\frac{C}{\varrho^3}\right)\mathbf{T}_\alpha{}^{-1}\mathbf{T}_\beta{}^{-1}\mathbf{S}\mathbf{T}_\beta\mathbf{T}_\alpha\vec{f}_{tx} \tag{5}$$

We calculate the vector $\vec{r}$ (as an unit vector) from the ratios of the components of the receiver signal vector $\vec{f}_{rx}$, for that reason the constant factor C/ϱ^3 in (5) is omitted.

III. Experimental Setup

In order to solve the localization task described by (5) in Section II, the receivers need the ability to measure the magnetic field in all three spatial directions at a defined position. This section discusses the design and the arrangement of the receivers as well as the measurement setup used to perform preliminary localization measurements.

A. Design of the reciver

We developed a receiver design with three coils where each of them are placed orthogonally to the other two (like shown in Figure 2) in order to measure the x-, y-, and z-components of the transmitter magnetic field at one point. The first version of the receiver electronic circuit was based on a LC-Tank tuned to the transmitter frequency. Therefore, each receiver coil was connected in parallel with a capacitor and a resistance. In

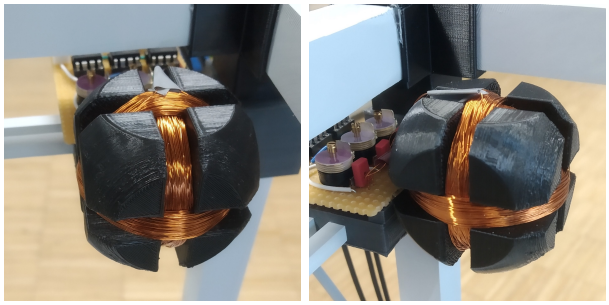

Figure 2. Receiver coils

contrast to the theory, the mutual inductances between the orthogonally placed coils are not zero in practice. The use of LC-Tanks as a main receiver architecture was therefore dismissed since they lead to mutual oscillations of the three oscillators because of the existing minimal mutual inductions. So, we choose to use an active resonant filter tuned to the transmitter frequency in order to amplify the signal which is inducted in each receiver coil. Figure 3 shows its circuit where the receiver coil would be connected to the pin V_{in}. The filter amplifies the signal at the resonant frequency by the gain factor of $|G| \approx 200$ as can be seen from its frequency response in Figure 4. In order to enable a manual calibration of the resonant frequency, the capacitor C_1 (see Figure 3) has been realized as a parallel connection of a variable capacitor and a fixed one. The resistance R_1 has been realized as a potentiometer to enable an adjustment of the gain factor.

B. Arrangement of the receivers

By calculating the angles α and β with (5), we get multiple possible solutions for the direction vector $\vec{r}$ per receiver. The

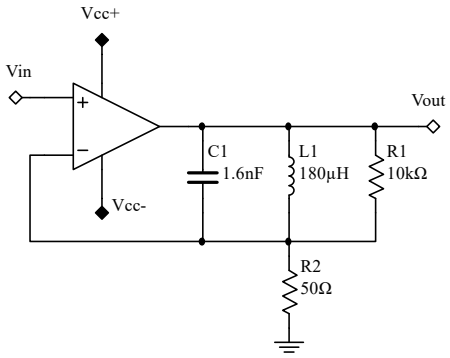

Figure 3. Active resonant filter

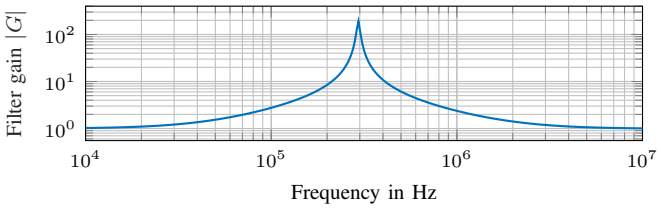

Figure 4. Frequency response of the active resonant filter

reason for that is the rotation symmetry of the magnetic field of a round coil. Positioning the receivers at crucial positions, the possible solutions can be diminished to one useful solution for each receiver. If the receiver is placed at a corner of the region of interest, the number of possible solutions for the direction vector is automatically diminished to one. Figure 5 shows the arrangement used for the first localization measurements. The

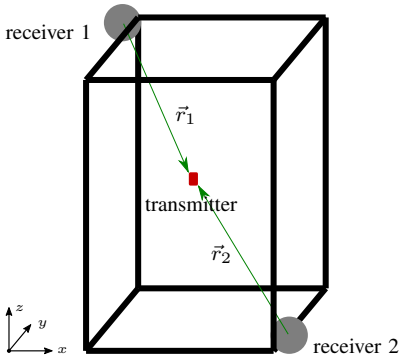

Figure 5. Receiver arrangement

receiver signals were digitalized with the *National Instruments USB6366* I/O device. The software *Matlab* by *MathWorks* is used to control the I/O device and for solving (5) in order to calculate the transmitter position.

IV. Measurement Results

We performed localization mesurements with a two receiver setup like shown in Figure 5. The height (z) and width (x) of our setup construction is 50 cm, the depth (y) is 30 cm. The setup is entirely made out of plastic materials in order to not influence the magnetic field. We performed measurements with the same x- and y-positions at different heights. The measured positions are compared to the exact ones in Figure 6 for a constant height of $z = 25$ cm. The maximum absolute errors per coordinate for the measurements shown in Figure 6 are:

- max abs. error x-coordinate = 3.9 cm
- max abs. error y-coordinate = 2.4 cm
- max abs. error z-coordinate = 4.7 cm

Figure 7 shows the mean values of all relative errors (x-, y-, and z-coordinates) referred to the test setup dimensions for different heights (the five x- and y-coordinates are the same at each height).

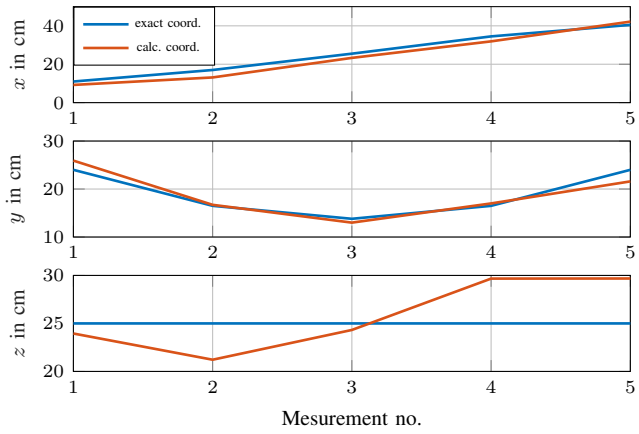

Figure 6. Exakt coordinates vs. measured coordinates

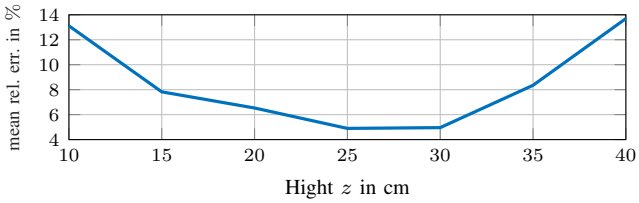

Figure 7. Mean values of the relative errors of all three coordinates at different heights

V. Simulation: Accuracy Improvement by Using Three or More Receivers

We performed preliminary simulations where the differences in accuracy were calculated between a two receiver setup and a setup with three or more receivers in order to get an idea about the improvement of the overall accuracy. We use *Matlab* by *MathWorks* to calculate the signal amplitudes in x-, y-, and z-direction for each receiver, for a given transmitter position. With the calculated amplitudes sinus signals where generated and three types of noise/signal interferences where added:

- variation of the signal amplitude
- overlap of the power supply magnetic field signal
- overlap of white noise

For the simulations no. 1 and 2 in Table I, the signal amplitude is varied using random values in the range between 0 and 5% of the calculated exact amplitude. White noise is added using random values in the range between 0 and 50% of the signal amplitude and the power supply signal is added with the same amplitude as the calculated clean receiver

 ISBN: 978-1-61208-819-8

signal amplitude. For the simulations no. 3 and 4, the signal amplitude is varied randomly in the range between 0 and 15%. The other parameters were left as for measurements no. 1 and 2. With these constrains the difference vector $\vec{d}$ between the calculated position and the exact position is determined for over 7000 transmitter positions in our region of interest shown in Figure 5. The third receiver is placed in the upper right corner over the receiver 2. The fourth receiver is placed in the lower front left corner and the fifth receiver in the upper back right corner of our region of interest. As a measure of accuracy we use the length of the difference vectors between the exact and the calculated positions. In Table I the mean values of the difference vector lengths of all measurements are listed for setups with two to five receivers. It can be seen that the length of the difference vectors decreases by more than half if the setup with two receivers is compared to the setup with three receivers. By using more than three receivers the improvement gets smaller.

TABLE I. MEAN VALUES IN CM OF THE DIFFERENCE VECTORS FOR THE TWO RECEIVER SETUP AND THE THREE RECEIVER SETUP

sim. no.	sig. ampli. variation	calc. pos.	mean $\lvert\vec{d}\rvert$ 2 rec.	mean $\lvert\vec{d}\rvert$ 3 rec.	mean $\lvert\vec{d}\rvert$ 4 rec.	mean $\lvert\vec{d}\rvert$ 5 rec.
1	max. 5%	7057	3.52 cm	1.55 cm	1.31 cm	1.02 cm
2	max. 5%	7057	3.51 cm	1.55 cm	1.29 cm	1.01 cm
3	max. 15%	7057	10.53 cm	4.62 cm	3.83 cm	3.09 cm
4	max. 15%	7057	10.38 cm	4.50 cm	3.89 cm	3.07 cm

VI. CONCLUSION

For the measurements described in Section IV, the major deviations from the exact position can be found in the z-coordinate. It can be seen from Figure 7 that the overall highest accuracy is reached at approx. half the height (z-coordinate) between receiver 1 and receiver 2. For low z-coordinates or for high z-coordinates the distance to one receiver gets bigger and the accuracy gets lower.

The feasibility of the method has been shown. The future aim is to improve the overall accuracy. We already showed in Section V that the inaccuracy can diminished by more then a half by using a third receiver.

The position of the transmitter is now calculated by evaluating the ratios of the components of the receiver signal vector $\vec{f}_{rx}$ individually for each receiver. In future, in order to improve the accuracy, the sum of the amplitudes will be compared between the receivers, this should yield additional information about the sensor position. The orientation of the receiver plays an important role on the overall accuracy of this system. For the case that the receiver is not aligned with the overall coordinate system, the coupling equation between the transmitter and the receiver has to be adopted by adding some more rotation matrices for the three receiver orientation angles. In future work our approach will be to calculate an optimization for the receiver orientation and position in order to minimize the susceptibility to overall inaccuracies. Imperfections in the orientation of the transmitter also leads to measurement inaccuracies. To counteract this problem, a solution could be the search for a minimum in the coupling equation expanded by the rotation matrices for a transmitter inclination using the position coordinates calculated with the (5) as initial values.

REFERENCES

[1] M. Heining, A. Sutor, S. Stute, C. Lindenberger, and R. Buchholz, "Internal illumination of photobioreactors via wireless light emitters: a proof of concept," Journal of Applied Phycology, vol. 27, 2015, pp. 59–66.

[2] A. Sutor, M. Heining, and R. Buchholz, "A class-e amplifier for a loosely coupled inductive power transfer system with multiple receivers," Energies, vol. 12, no. 6, 2019.

[3] B. O. Burek, A. Sutor, D. W. Bahnemann, and J. Z. Bloh, "Completely integrated wirelessly-powered photocatalyst-coated spheres as a novel means to perform heterogeneous photocatalytic reactions," Catal. Sci. Technol., vol. 7, no. 21, 2017, pp. 4977–4983.

[4] T. Lauterbach et al., "Sens-o-spheres – mobile, miniaturisierte sensorplattform für die ortsungebundene prozessmessung in reaktionsgefäßen," 13. Dresdner Sensor-Symposium 2017, Hotel Elbflorenz, Dresden, 12 2017, pp. 89 – 93.

[5] D. Demetz, O. Zott, and A. Sutor, "Wireless and traceable sensors for internally illuminated photoreactors," in 2020 IEEE International Conference on Industrial Technology (ICIT), 2020, pp. 582–586.

[6] M. C. Domingo, "Magnetic induction for underwater wireless communication networks," IEEE Transactions on Antennas and Propagation, vol. 60, no. 6, June 2012, pp. 2929–2939.

[7] U. M. Qureshi et al., "Rf path and absorption loss estimation for underwater wireless sensor networks in different water environments," Sensors, vol. 16, no. 6, 2016.

[8] X. Che, I. Wells, G. Dickers, P. Kear, and X. Gong, "Re-evaluation of rf electromagnetic communication in underwater sensor networks," IEEE Communications Magazine, vol. 48, no. 12, December 2010, pp. 143–151.

[9] Y. Li, H. Yin, X. Ji, and B. Wu, "Design and implementation of underwater wireless optical communication system with high-speed and full-duplex using blue/green light," in 2018 10th International Conference on Communication Software and Networks (ICCSN), July 2018, pp. 99–103.

[10] J. Shi, S. Zhang, and C. Yang, "High frequency rf based non-contact underwater communication," in 2012 Oceans - Yeosu, May 2012, pp. 1–6.

[11] F. H. Raab, E. B. Blood, T. O. Steiner, and H. R. Jones, "Magnetic position and orientation tracking system," IEEE Transactions on Aerospace and Electronic Systems, vol. AES-15, no. 5, Sep. 1979, pp. 709–718.

 ISBN: 978-1-61208-819-8